Supplementary Information

Interface Intercalation into Perovskite Layer Improving Performance of Tin Perovskite Solar Cells

Muhammad Okash Ur Rehman[1†], Debendra Prasad Panda[1†], Wolfram Hempel[2], Rabeb Issaoui[1], Madineh Rastgoo[1], Alwani Imanah Rafieh[3], Valerio Stacchini[3], Lorenzo Miele[1], Enrica Luzzi[1], Luigi Sanguigno[1], Paolo Aprea[1], Meng Li[4], Guixiang Li[5], Zafar Iqbal[3]*, and Antonio Abate[1,3]*

[1]*Department of Chemical, Materials and Industrial Production Engineering, University of Naples Federico II, 80125 Naples, Italy.*

[2]*Zentrum für Sonnenenergie und Wasserstoff-Forschung Baden-Württemberg (ZSW) Meitnerstraße 1 70563Stuttgart, Germany.*

[3]*Solar Energy Divison, Helmholtz-Zentrum Berlin für Materialien und Energie (HZB) Hahn-Meitner-Platz 1, 14109 Berlin, Germany.*

[4]*Key Lab for Special Functional Materials of Ministry of Education, School of Nanoscience and Materials Engineering, Henan University, Kaifeng, 475004 China.*

[5]*School of Materials Science and Engineering, Southeast University, Nanjing, 211189, Jiangsu, China.*

[†]Authors contributed equally

*Corresponding Authors

Zafar Iqbal, Email: zafar.iqbal@helmholtz-berlin.de

Antonio Abate, Email: antonio.abate@unina.it ; antonioabate83@gmail.com

Materials and Devices

Chemicals:

ITO was purchased from Suzhou ShangYang Solar Technologgy Co.,Ltd. Water-free PEDOT complex dispersion in toluene (HTL3) was obtained from CleviosTM. Formamidinium iodide and Phenylethylammonium iodide were purchased from Dyenamo. 2-Pyridyl thiourea was purchased from Thermo Fisher Scientific. Silver shot (1–5 mm, 99.9%) was supplied by Alfa Aesar, and C_{60} was procured from CreaPhys. All other chemicals, including SnI_2, DEF (N,N-Diethylformamide), DMPU (N,N′-Dimethylpropyleneurea), toluene, Al_2O_3, ethanol, diethyl ether (DEE), Bathocuproine (BCP), and ethylenediammonium diiodide ($EDAI_2$) were obtained from Sigma-Aldrich and used without further purification.

Device Fabrication:

The patterned ITO substrates (2.5 x 2.5 cm², 10 Ohms per square) were cleaned using a 2% Hellmanex solution in deionized (DI) water, followed by sequential washes with DI water, acetone, and isopropyl alcohol for 15 minutes each at 40 °C. After thorough drying, the substrates underwent UV-ozone treatment for 15 minutes at 35 °C. Immediately following the UV-ozone treatment, the cleaned substrates were transferred into a nitrogen-filled glovebox. It is important to note that all fabrication steps were conducted within a high-purity nitrogen-filled glovebox (temperature around 18 °C) that had never been exposed to dimethyl sulfoxide (DMSO). Solvent regeneration was frequently performed to prevent solvent vapor accumulation. A freshly prepared PEDOT complex, diluted in dry toluene (1:6 v:v) was spin-coated onto the substrates at 500 rpm for 5 seconds, followed by 4000 rpm for 40 seconds. The films were then annealed at 150 °C for 10 minutes. Freshly prepared Al_2O_3 nanoparticle solution diluted in dry ethanol (1:50 v:v) was spin-coated onto the substrates followed the same program and then annealed at 100 °C for 5 minutes.[1] For PEAI modification 0.5 M solution of $PEAI_2$ in DEF:DMPU (6:1 v:v) was spin coated using the same program. The stock solutions of SnI_2 (1.2 M) and $EDAI_2$ (1 M) were prepared in a DMSO-free solvent system consisting of N,N-diethylformamide and N,N'-dimethylpropyleneurea (DEF:DMPU, 6:1 v:v), and left overnight in a thermoshaker at 19 °C before the final perovskite solution preparation. The

$FASnI_3$ solution (1.2 M in DEF:DMPU with 10% SnI_2 over stoichiometry, 10% of 0.1M solution of 2-Pyridyl thiourea and 5% $EDAI_2$ additives) was spin-coated at 500 rpm for 5 seconds and 4000 rpm for 40 seconds. After 22 seconds of spinning, 100 µL of diethyl ether (DEE) was dropped onto the substrate to induce crystallization, followed by annealing at 100 °C for 30 minutes. As the electron selective contact, C_{60} (40 nm) and BCP (7 nm) were sequentially evaporated under a vacuum of 10^{-6} mbar, with deposition rates ranging between 0.1 and 0.3 Å/s. Silver was then evaporated through a shadow mask at an initial rate of 0.1 Å/s up to 10 nm, increasing to 0.2 Å/s up to 20 nm, and finally 1 Å/s up to 140 nm. The final device area was approximately 0.17 cm^2. Devices were stored in the glovebox until measurement. 10%

Characterizations:

X-ray diffraction (XRD): The Powder XRD was conducted using the PANalytical instrument (Cu $K\alpha_1$ and $K\alpha_2$ radiation) incorporated with a PIXcel1D detector.

Scanning Electron Microscopy (SEM): SEM measurement was conducted using FEI Quanta 200 FEG instrument. Top surface SEM measurement was conducted on the films (ITO/PEDOT-complex/Al_2O_3/$FASnI_3$, 2D/ $FASnI_3$).

Photoluminescence (PL) Spectroscopy: To measure the PL signal a commercial platform (Arkeo-Ariadne, Cicci Research s.r.l.) were used inside the N_2 filled glovebox using. The substrate was irradiated at an angle of 45° using a diode-pumped solid-state Nd/YVO_4 + KTP laser (peak wavelength: 532 ± 1 nm; optical power: 1 mW on a 2 mm diameter circular spot, resulting in an intensity of 31 $mWcm^{-2}$). The substrate was illuminated on the one side and resulting fluorescence was directed towards a 10 mm diameter fiber bundle. The aspheric lens was strategically positioned in close proximity to the substrate to ensure optimal collection of PL. Subsequently, the signal was directed towards a CCD based spectrometer for analysis. In order to facilitate a more robust comparison of the results, the illumination time and averaging parameters were kept at their original levels.

Transient surface photovoltage (tr-SPV) measurements for $FASnI_3$ Perovskites: Charge extraction dynamics were investigated by non-contact transient surface photovoltage (tr-SPV) measurements spanning the time domain from 5 ns to 0.1 s. Samples were excited using a by a pulsed laser system equipped with a wavelength-tunable output, with a spectral

range adjustable from 1.0 to 2.0 eV in increments as fine as 0.01 eV. The excitation beam was focused to a fixed 5 mm spot size, and its intensity was modulated using calibrated filters. For the measurements reported here, the laser was operated at maximum output intensity exceeding 10 suns equivalent, enabling detection of SPV signals even in tin-based halide perovskites (HaPs), where high recombination rates typically suppress signal levels. Measurements were performed using a fluence of 72 µJ/pulse to track energy-resolved charge extraction and identify onset features around 1.4 eV in $FASnI_3$. No laser-induced degradation was observed under these conditions. To prevent ambient-induced sample degradation, all films were encapsulated in nitrogen atmosphere (e.g., with UV-curable epoxy and glass) immediately after fabrication and prior to SPV analysis. Full experimental setup details are available in previous studies.[2,3]

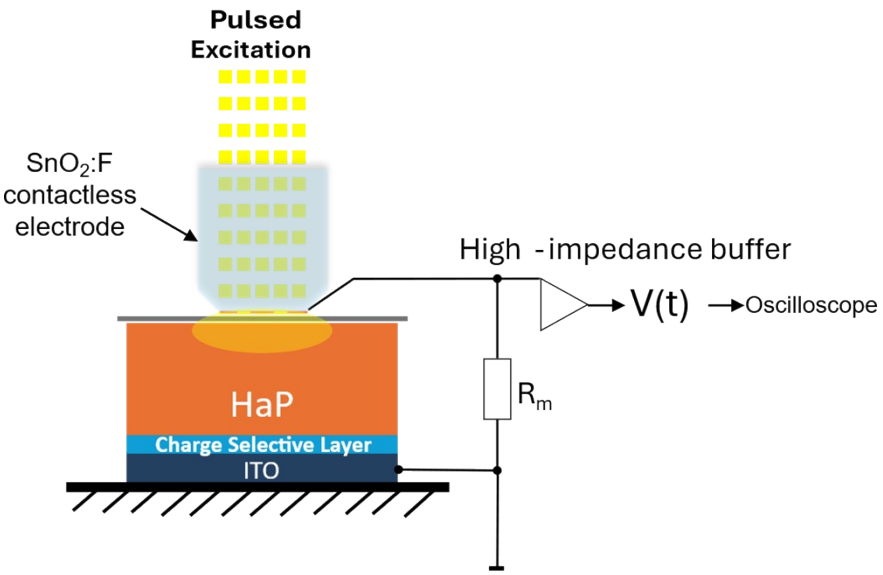

Time-resolved photoluminescence (trPL) measurements:

Time-resolved photoluminescence (trPL) was conducted using a custom-built confocal photoluminescence (PL) setup in air on the encapsulated samples. To effectively separate the excitation and detection paths the setup incorporated with an ‘‘80:20’’ - ‘‘transmission-reflection’’ beam splitter. A SuperK FIANIUM white light laser source was employed for excitation, delivering the light within the 545-555 nm spectral range at 153 kHz repetition rate. The laser beam was filtered by a Thorlabs FESH0650 (650nm shortpass) filter. The energy of the laser beam was adjusted to ≈2 µW by employing a linear-gradient neutral density filter. The focus and PL collection have been facilitated by an off-axis parabolic mirror with a focal

length of 5 cm. The laser spot diameter is approximately 120 µm. A silicon single-photon avalanche diode (Laser Components COUNT50) was utilized for the detection of PL, with subsequent signal modulation facilitated by a 650-nm long-pass filter (FELH650, Thorlabs). The PL count and decay histogram were acquired using a Picoquant TimeHarp260 Nano TCSPC module.

The decay curves are fitted using the the biexponential equation:

$$I_t = I_0 + A_1 e^{-\frac{t}{\tau_1}} + A_2 e^{-\frac{t}{\tau_2}}$$

Here τ_1 and τ_2 are lifetimes of two different decay channels contributing to the emission process. The average lifetimes (τ_{av}) were calculated using the formula:

$$\tau_{av} = \frac{A_1\tau_1^2 + A_2\tau_2^2}{A_1\tau_1 + A_2\tau_2}$$

Time of flight secondary ion mass spectrometry (ToF-SIMS): ToF-SIMS measurements were run on a ToF-SIMS5 from Iontof. The analysing beam Bi^+ (30 keV) raster an area of 50x50 µm2. The Cs-gun (1 keV) was chosen for sputtering with a crater size of 250x250 µm2. The use of the Cs-gun offered the possibility to measure Cs cluster as for instant CsI^+ for a good detection of positive and negative Ions in the same measurement.

Space-charge-limited current (SCLC): Hole-only devices were fabricated for the space-charge-limited current (SCLC) measurements. The perovskite films made on the PEDOT-coated substrates were spin-coated with 150 µL PTAA solution (20 mg mL^{-1} in chlorobenzene) at 2000 rpm for 30 s and annealed at 65 °C for 5 minutes. For the top electrode 100 nm of silver was evaporated using a metallic aperture mask. Characterization was performed inside N_2 filled glovebox under dark conditions.

The trap density (N_t) was calculated using this formula.

$$N_t = \frac{2\varepsilon_r\varepsilon_0 V_{TFL}}{eL^2}$$

Where ε_r for both control and target were kept constant (8.5). ε_0 is permittivity of free space (8.854×10^{-12} F/m). e is elementary charge (1.602×10^{-19} C).

Photovoltaic Performance:

The J-V curves were measured inside the glovebox by a commercial apparatus Arkeo-Ariadne by Cicci Research s.r.l. based on a ring of 12 LEDs covering the wavelengths from 300 to 1000 nm calibrated to fit class A and using of 4-wire source meter. For the measurement of incident photon-to-current efficiency (IPCE) spectrum was recorded using another commercial system Arkeo-Ariadne Cicci Research s.r.l. system based on 300-Watt xenon lamp to read the spectrum in the range from 300 to 1000 nm.

Figures:

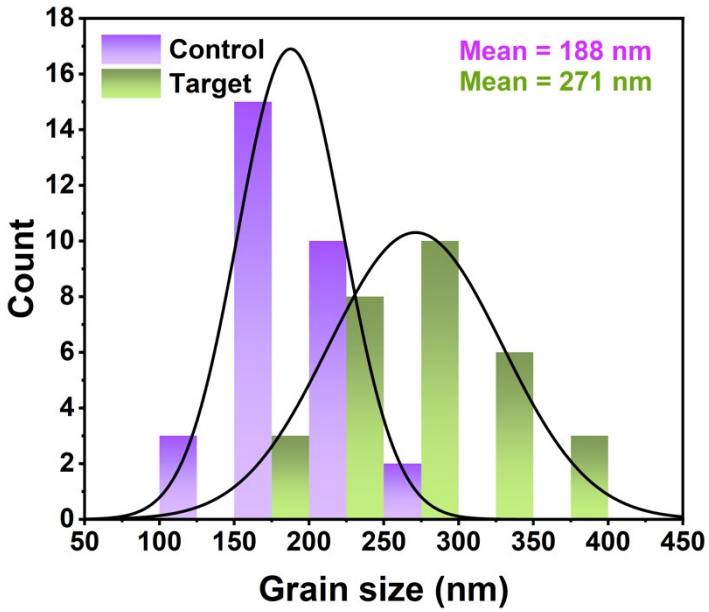

Figure S1. Statistical studies showing target films exhibit better microstructure with larger grains.

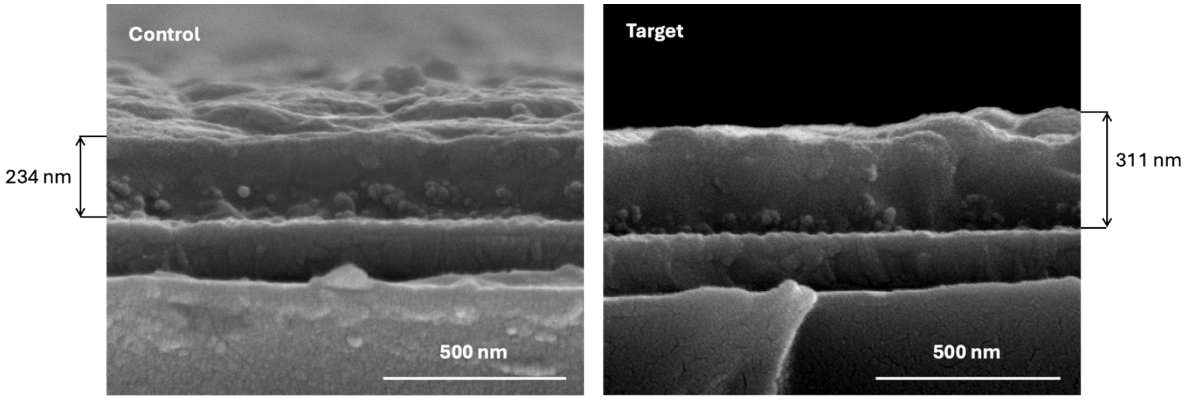

Figure S2. Cross-sectional SEM images for the PSCs. (a) control ($FASnI_3$) (b) target ($PEAI/FASnI_3$).

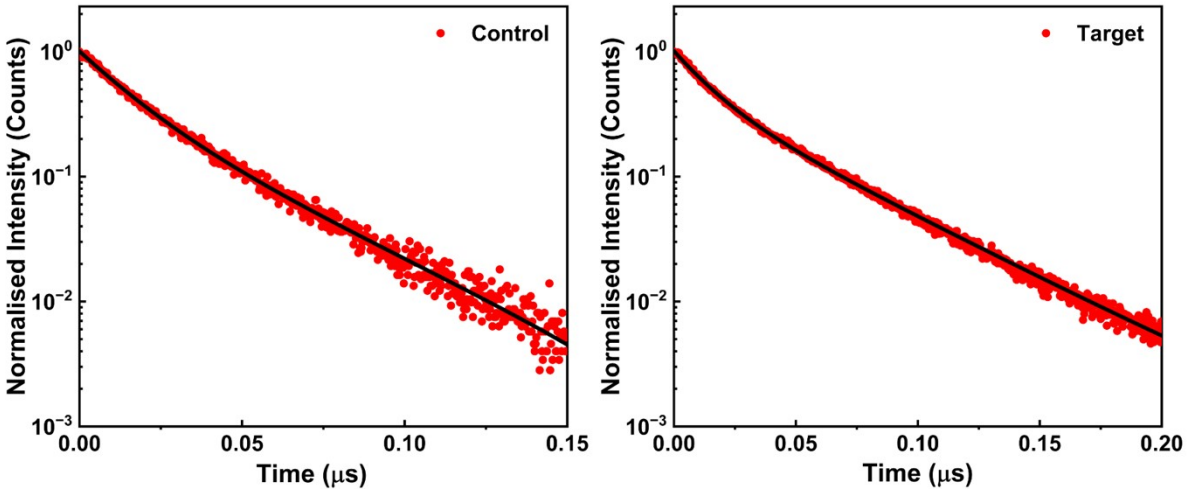

Figure S3. Time-resolved photoluminescence (trPL) decay spectra of control ($FASnI_3$) and target ($PEAI/FASnI_3$) films fitted with biexponential equation.

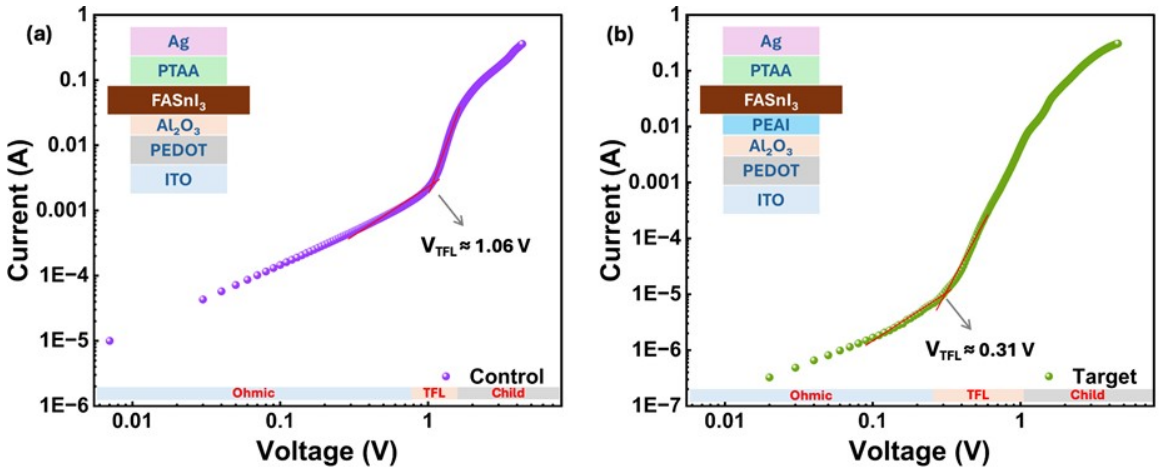

Figure S4. SCLC measurements of hole-only devices based on the perovskite films (a) control and (b) target

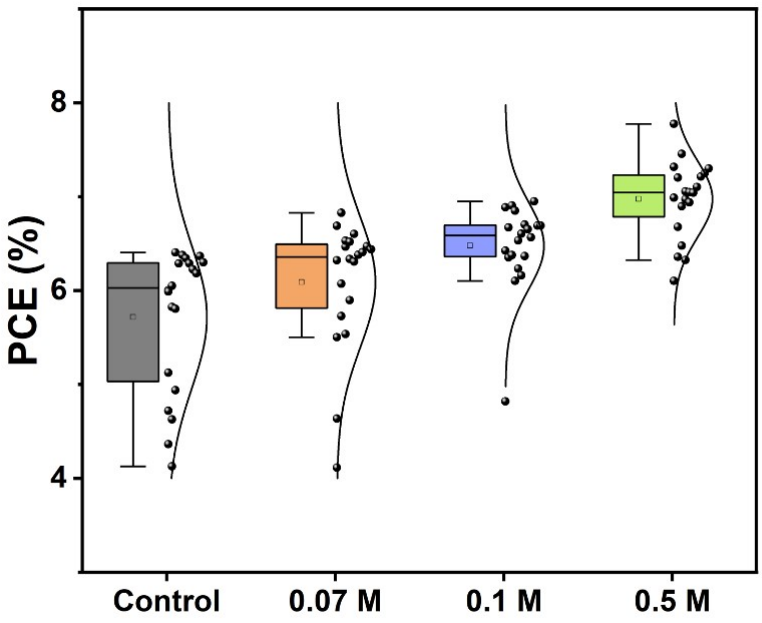

Figure S5. PCE of control and different molar concentration of PEAI devices under AM 1.5G light illumination.

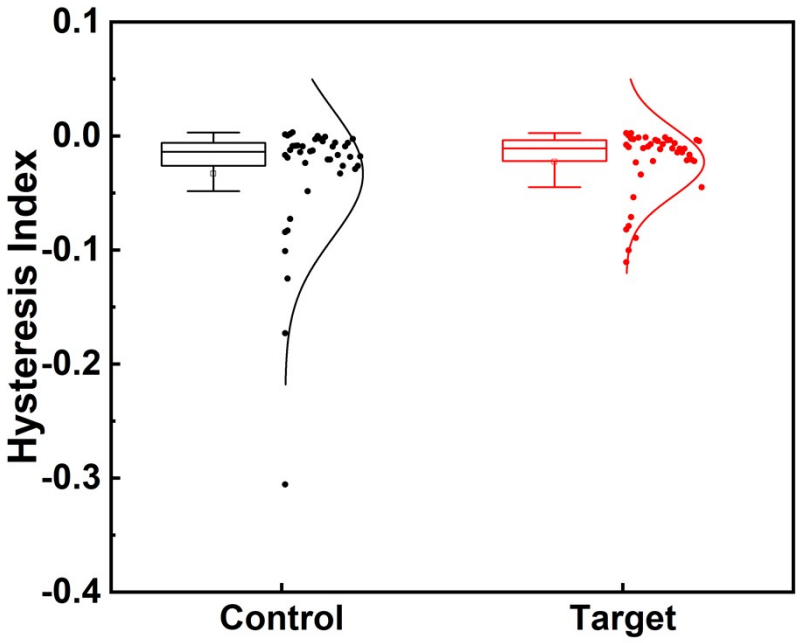

Figure S6. A comparison of the hysteresis index (HI) of control ($FASnI_3$) and target ($PEAI/FASnI_3$) perovskite cells.

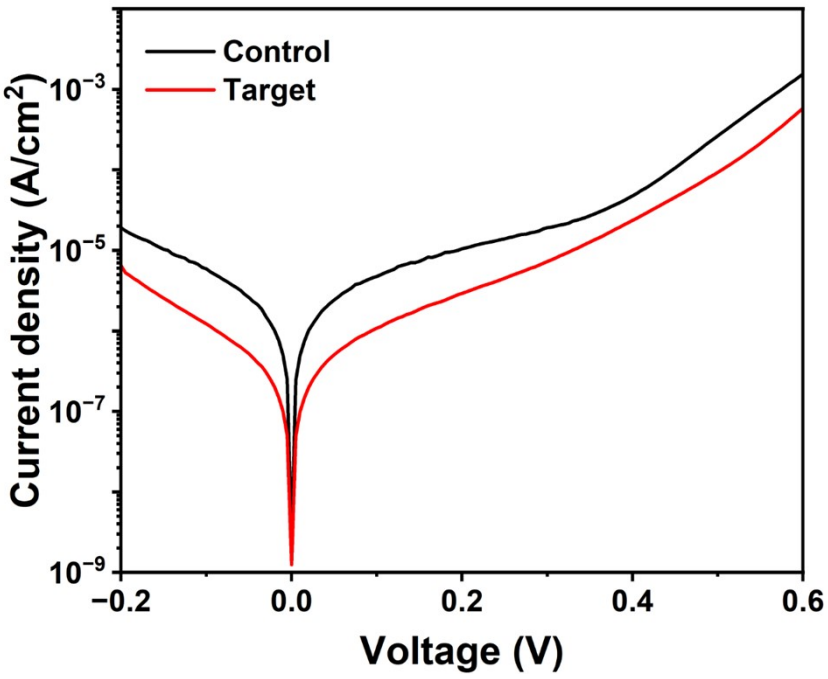

Figure S7. J-V curves of control ($FASnI_3$) and target (PEAI/$FASnI_3$), perovskite solar cell under dark condition.

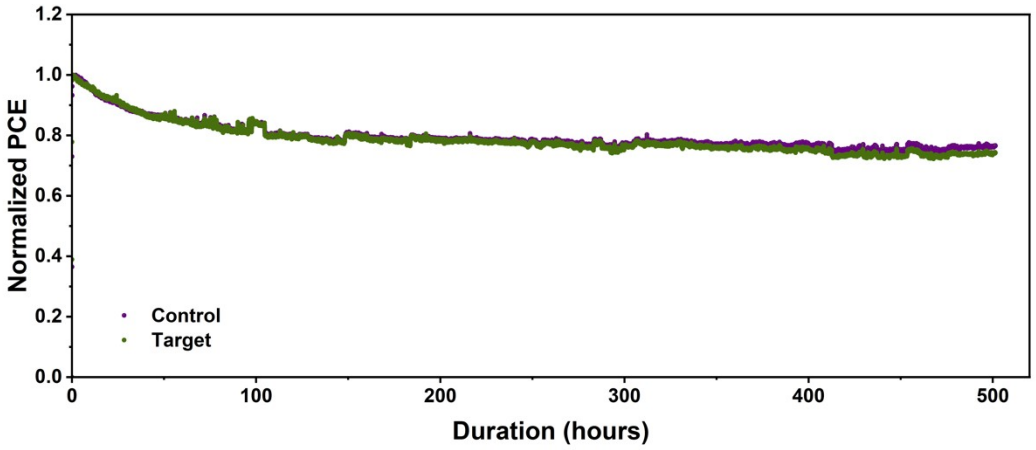

Figure S8. Long-term stability under continuous 1-sun illumination for 500 hours.

Tables:

Table S1. Full-width at half maxima of the (100) XRD peak of $FASnI_3$ and PEAI/ $FASnI_3$.

Perovskite	**FWHM (º)**
Control	0.123
Target	0.115

Table S2. Photovoltaic performance of $FASnI_3$ and PEAI/ $FASnI_3$ based champion devices under AM 1.5G light illumination.

Device	Scan	Voc (V)	Jsc (mA/cm^2)	FF (%)	PCE (%)
Control	Forward	0.60	21.4	70	8.9
Target	Forward	0.69	21.3	75	11

Table S3. Highest reported PCE (%) for DEF:DMPU-based tin perovskite solar cells (year-wise).

Year	PCE (%)	References
2021	6.2	[4]
2022	7.5	[1]
2023	8.7	[5]
2024	7.7	[6]
2025	9.1	[7]
2025	8.1	[8]
2026	11	This Work

References

1 D. Di Girolamo, E. Aktas, C. Ponti, J. Pascual, G. Li, M. Li, G. Nasti, F. Alharthi, F. Mura and A. Abate, *Mater. Adv.*, 2022, **3**, 9083–9089.

2 S. Mariotti, E. Köhnen, F. Scheler, K. Sveinbjörnsson, L. Zimmermann, M. Piot, F. Yang, B. Li, J. Warby, A. Musiienko, D. Menzel, F. Lang, S. Keßler, I. Levine, D. Mantione, A. Al-Ashouri, M. S. Härtel, K. Xu, A. Cruz, J. Kurpiers, P. Wagner, H. Köbler, J. Li, A. Magomedov, D. Mecerreyes, E. Unger, A. Abate, M. Stolterfoht, B. Stannowski, R. Schlatmann, L. Korte and S. Albrecht, *Science*., *381*, 63–69 (**2023**).

3 I. Levine, A. Al-Ashouri, A. Musiienko, H. Hempel, A. Magomedov, A. Drevilkauskaite, V. Getautis, D. Menzel, K. Hinrichs, T. Unold, S. Albrecht and T. Dittrich, *Joule*, 2021, **5**, 2915–2933.

4 D. Di Girolamo, J. Pascual, M. H. Aldamasy, Z. Iqbal, G. Li, E. Radicchi, M. Li, S. H. Turren-Cruz, G. Nasti, A. Dallmann, F. De Angelis and A. Abate, *ACS Energy Lett.*, 2021, **6**, 959–968.

5 E. Aktas, I. Poli, C. Ponti, G. Li, A. Olivati, D. Di Girolamo, F. A. Alharthi, M. Li, E. Palomares, A. Petrozza and A. Abate, *ACS Energy Lett.*, 2023, **8**, 5170–5174.

6 S. Covella, V. Armenise, M. O. Ur Rehman, E. Aktas, F. Fracassi, F. Palumbo, S. Colella, A. Abate, A. Listorti, *ACS Appl. Mater. Interfaces* **2024**, *37*, 49392.

7 M. Zhu, S. Singh, A. M. C. Chong, J. M. Kim, F. Koc, D. P. Panda, P. Zimmermann, A. Hinderhofer, W. Luo, G. Alsabeh, M. O. Ur Rehman, G. Choi, D. Chernyshov, F. Schreiber, J. Y. Seo, Y. Vaynzof, A. Abate and J. V. Milić, *Adv. Energy and Sustain. Res.* **2025**, 202500028.

8 D. P. Panda, R. Issaoui, Z. Iqbal, G. K. Grandhi, M. O. Ur Rehman, F. Zu, P. Alippi, M. Rastgoo, S. Zuo, E. Luzzi, M. Simmonds, L. Miele, L. Sanguigno, M. Li, P. Aprea, E. Di Maio, N. Koch, P. Vivo and A. Abate, *ACS Energy Lett.* 2025, **10**, 3789−3798.